Autofocusing synthetic aperture radar images

C. Prati

ABSTRACT

Correct focusing of Synthetic Aperture Radar data depends upon knowing both the geometric and transmission parameters of the system precisely. Transmission parameters (i.e. transmitted wavelengths, pulse repetition frequencies, sampling rate, etc.) are generally defined specifically, whereas geometric parameters such as sensor- target relative positions, satellite velocities, attitude etc. can be derived from the satellite effemerides or data. Referring to the focusing technique described by Rocca (1987), the only two geometric parameters involved in the focusing process are the sensor-target relative velocity and the sensor-target closest approach distance. In this paper, we suggest a technique to extract these two geometric parameters from the data themselves (autofocusing) in order to achieve the best possible focusing of SAR images. This technique has been tested both on synthetic and on real SEASAT and SIR-B data. The achieved precision of the parameters value has been estimated to be better than one part over ten thousand.

INTRODUCTION

Synthetic Aperture Radar (SAR) is a remote sensing technique that uses electromagnetic waves with a frequency normally ranging between 1 and 10 GHz (L,C and X band). The system is, essentially, a conventional radar with an antenna a few meters large; the system takes advantage of its relative motion with respect to the target to achieve a satisfying spatial resolution in the along-track direction (azimuth). Referring to the SEASAT data (Fitch, 1988), for example, the distance between the sensor and the target is about 800Km; the transmitted wavelength is 23 cm; and the antenna size is 10 m. With such parameters, a conventional radar would have a spatial resolution in the azimuth direction of about 20 km. Taking advantage of the sensor-target relative motion, the system can provide a spatial resolution up to 6 m.

Such high resolution can only be achieved by accurate processing of the SAR raw data. A simple and almost exact way to process SAR data is to apply the wave equation (Rocca; 1987). The resulting algorithm can efficiently handle data which lie along the correct range-varying hyperbolic arrival times curve. A precise knowledge of the survey system parameters is necessary to make the algorithm work properly. The transmission parameters (i.e. the transmitted wavelength, the pulse repetition frequency, the sampling rate etc.) are generally known precisely. The geometric ones, on the other hand, (i.e. sensor-target relative position, satellite velocity and attitude etc.) can be derived from the effemerides of the satellite or from the data itself (autofocusing). The second solution is preferable for at least two reasons:

i) The geometric parameters used in the processing have different values from those which are derived from the satellite effemerides because of the effect of the orbit curvature.

ii) The measurement of the satellites' effemerides takes a long time to do accurately. This could be a problem for real-time on-board processing.

This paper presents a very precise autofocusing technique for SAR image processing.

AUTOFOCUSING PARAMETERS

Referring to the focusing technique described by Rocca (1987), the only two geometric parameters involved in the focusing process are the sensor-target relative velocity v and the sensor-target closest approach distance z_0. To understand how these two parameters are involved in the focusing process, let us refer to the simple system geometry of Figure 1. (The satellite trajectory is considered straight).

Using this geometric model the focused image can be derived from the raw data, or better, from its 2-D Fourier transform as:

$$d(x,-T_0,z) = \int\int d(k_x, c/2\sqrt{k_x^2+k_z^2} - \omega_0)c/2\frac{k_z}{\sqrt{k_x^2+k_z^2}} \qquad (1)$$

$$e^{-j(\frac{cT_0}{2}(\sqrt{k_x^2+k_z^2}-k_z))}e^{j(k_x x+k_z z)}dk_x dk_z \ .$$

From (1) the change of variable of the 2-D Fourier transform of the raw data depends only upon the platform velocity v (the spatial sampling rate and therefore k_x depends on v). The complex exponential term contains both the platform velocity and the closest approach distance: $z_0 = cT_0/2$ (The effect of the second term of the double integral is an amplitude correction which can be neglected for such a small angular aperture of the antenna). It can be shown that the change of variable of the raw data Fourier transform has no effect upon the focusing quality of the closer sources, whereas its effect becomes more sensible as the sensor-source distance

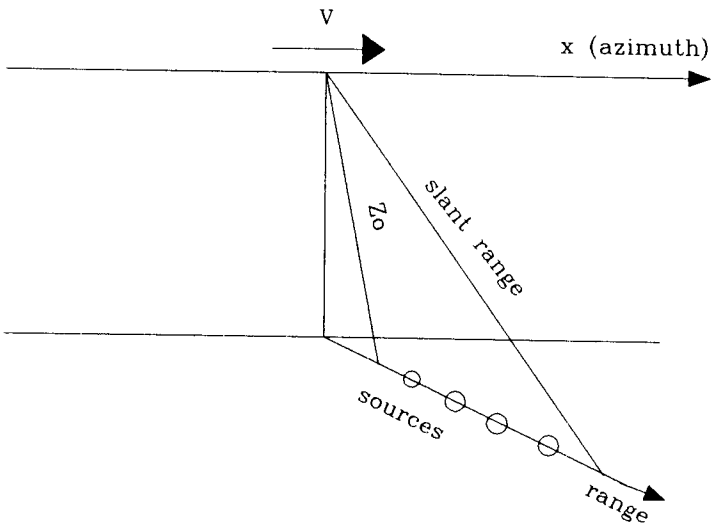

FIG. 1. SAR geometry.

increases. In other words, this change of variables compensates for the focusing parameters' variation resulting from the different range position of the observed sources. If we consider the very special case of only one active source on a black background, it is in fact very easy to focus this data set in the x,t domain by compensating for the different arrival times, and by applying a pure phase matched filter. Transforming this procedure in the k_x,ω domain, we obtain an integral expression that is identical to (1) but with a change of variable in $d(k_x,\omega)$.

Autofocusing in a small range interval

So far, we have shown that the change of variable in equation (1) can be neglected if we are considering sources that lie along a line parallel to the platform trajectory. In practice we can relax this condition by saying that the change of variable in equation (1) has no sensible effects upon the focused image until the sources are within a strip of terrain parallel to the platform trajectory. To quantify the maximum dimension of this strip, let us compute the variation within the range of the geometric parameters involved in the focusing process. Without loss of generality, we can refer to the simple geometry shown in Figure 2, where the plane that contains the platform trajectory and slant range axis is shown.

The arrival times equation for a source lying at a distance z from the platform trajectory is:

$$c^2\tau^2 = z^2 + x^2 = z^2 + v^2t^2. \tag{2}$$

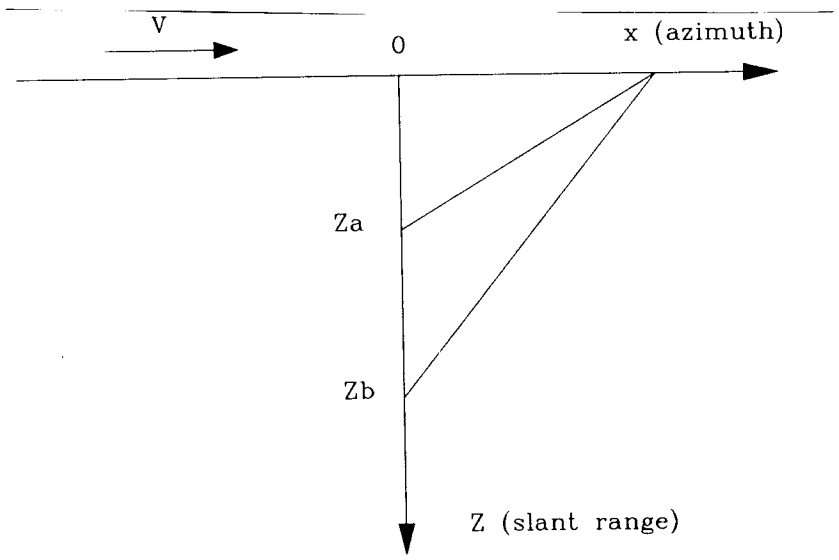

FIG. 2. Simplified SAR geometry.

Computing the second derivative of the arrival times τ with respect to time t at time $t = 0$, the following expression then holds:

$$z d^2\tau/dt^2 = v^2/c^2 \tag{3}$$

Experiments on synthetic and SEASAT data have shown that a variation of about 1 part over 1000 of the arrival times' second derivative can be considered the upper limit for a correct processing without parameter updating. In this case, it is easy to compute the maximum slant range interval Δz from equation (3):

$$\delta z = \frac{z}{\tau"}\delta\tau". \tag{4}$$

For the SEASAT data, the maximum slant range interval delta z is about 1 Km.

From equation (1), it is easy to see that if this limit is respected, the only geometric parameter involved in the focusing process is the second derivative of the arrival times. In fact, since the change of variable in (1) has no sensible effect on such a small range interval, the focusing process is thus essentially performed by the complex exponential term. The two geometric parameters v and z_0 are present in this term as a their combination which is proportional to $1/\tau"$.

Autofocusing in a large-range interval

If the range interval exceeds the limit imposed by equation (4), it is necessary to estimate both geometric parameters to process the entire image correctly. This goal can be reached by again taking advantage again of equation (3). In fact, we can

estimate the second derivative of the arrival times for two different range intervals centered, for example, on the sources a and b of Figure 2. Noting that the platform velocity v must be the same for all the sources, we can then derive the following equation:

$$z_a \tau_a" = z_b \tau_b". \tag{5}$$

Now, because the difference between z_a and z_b (Δz) is known perfectly (we have chosen it), we can solve equation (5) with respect to z_a, obtaining:

$$z_a = \frac{\tau_a" \Delta z}{\tau_b" - \tau_a"} \tag{6}$$

and

$$v^2 = \frac{z_a}{\tau_a"}. \tag{7}$$

Looking at equation (6), it can be noted that both $\tau_b"$ and $\tau_a"$ should be known precisely so as to produce a useful estimates of the parameter z_a (the closest approach distance). Consider the SEASAT data as an example. The ratio $\mu = \tau_b"/\tau_a"$ computed for a distance Δz = 20Km has a value very close to 1 (1.024). It is the result of the ratio between two numbers much greater than 1 (approx. 65). An error of 1 part over 1000 on the value of $\tau"$ produces an error of about 4 parts over 100 of the estimated closest approach distance z_a. Furthermore, the largest possible distance Δz should be used in order to fine-tune the precision. Referring to the previous example, and using the distance Δz= 50Km instead of 20Km, the error on z_a reduces to 1.5 parts over 100. In the following discussion we show an autofocusing technique that allows us to know the value of $\tau"$ with a precision of at least 1 part over 10000.

BLIND DECONVOLUTION

In the section above we identified the parameter that we need to estimate to correctly focus SAR data. Here we discuss how to estimate it from the data themselves.

Our problem is really simpler than in other applications; for example in reflection seismology, because we don't need to estimate all the impulse response of the system, but only one parameter. An easy, natural way to seek a solution is to focus the same raw data with a set of different parameter values, and to then evaluate which among them has produced the best-focused image. It is obvious that this is not a solution itself, since another question arises: How is optimal focusing identified? One possible solution is to define an objective function that has a maximum (or a minimum) in correspondence of the best focusing.

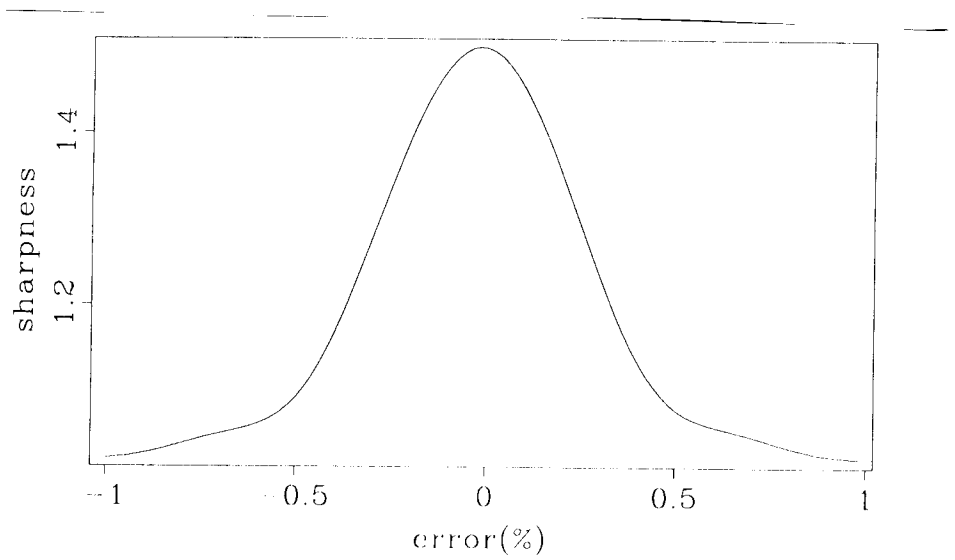

FIG. 3. Sharpness of the impulse response (ratio between the amplitude of the central lobe and the amplitude of lateral lobes) vs. the focusing parameter error.

Minimum Entropy Deconvolution

We first tested an objective function that takes advantage of the different statistical properties of focused and unfocused SAR data. SAR raw data have an almost complex Gaussian distribution, whereas the correctly deconvolved ones have a non-Gaussian nature. The focusing process can be regarded as a filter which transforms each hyperbola in the wavefield into a sharp spike, thereby changing the statistical distribution of the data. As shown in Figure 3, the sharpness of the impulse response, i.e. the ratio between the amplitude of the main lobe and the amplitude of lateral lobes, decreases with increasing focusing error.

The best focusing is that which produces the sharpest spikes; in other words, it is that which maximizes the distance between the statistical distribution of the filtered data and the Gaussian one. A possible objective function that increases with the distance from the Gaussian distribution is the "Kurtosis" introduced by Wiggins (1977). The Kurtosis has been computed on SEASAT SAR images focused with different satellite velocities, assuming a reasonable value of the satellite slant distance z_0. This data set was taken during a passage over the town of Reggio Calabria in southern Italy.

The defocusing effect due to the incorrect velocities can be clearly identified by visual inspection of the focused images shown in Figure 4.

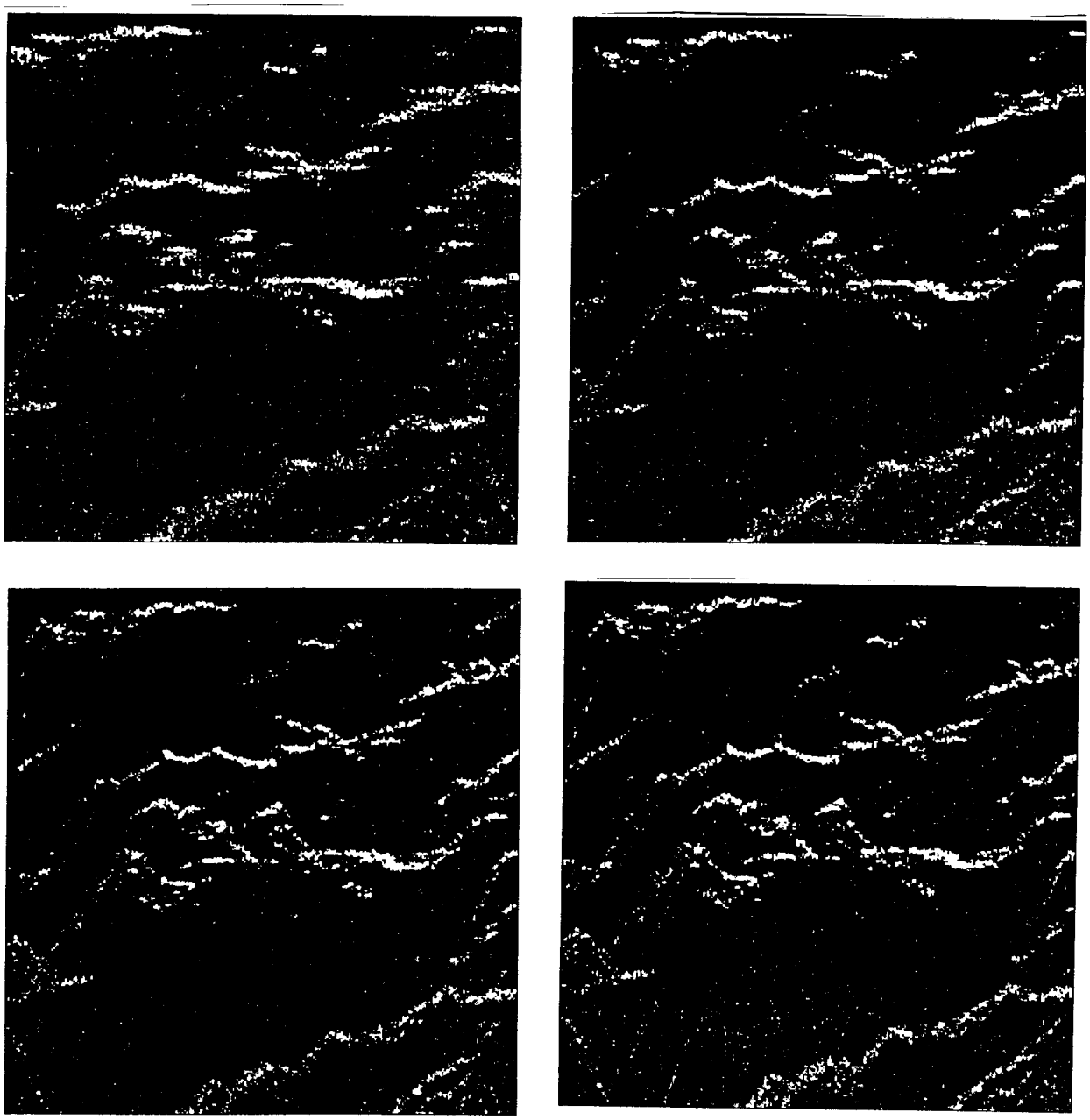

FIG. 4. Enlarged details of a SEASAT SAR image focused with different satellite velocities: a) $v = 7140$m/s, b)$v = 7180$m/s, c)$v = 7195$m/s, d)$v = 7205$m/s.

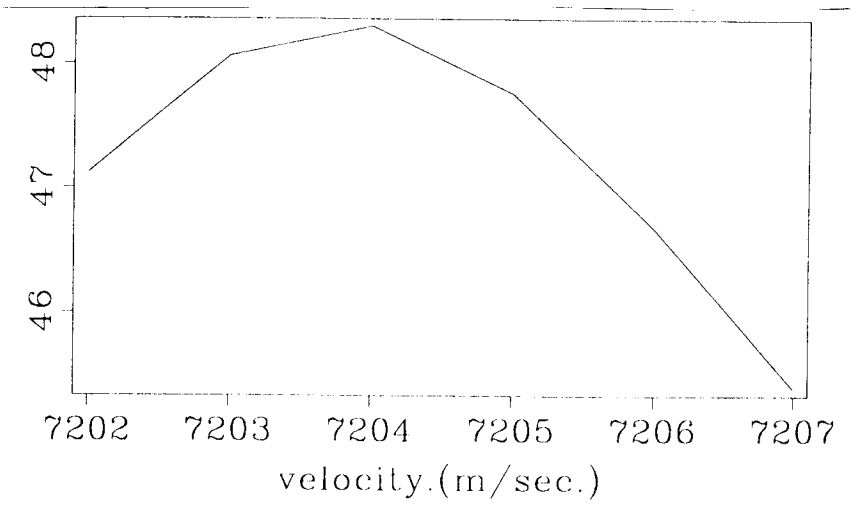

FIG. 5. Kurtosis vs. satellite velocity. Measure has been estimated from a SEASAT image (4096x256).

Nonetheless, it is not easy to judge the focusing quality variation when the change of the velocity is less than 2 parts over 1000. (In our case 15m/sec.). On the contrary, the Kurtosis shows a sensitivity which is better than one part over 10,000, as shown in the plot of Figure 5. The velocity value that corresponds to the maximum of the Kurtosis is clearly within the range of velocities that produced the best-focused images (as judged by visual inspection). Nevertheless, its consistency must be proven in some other way.

The same measurements have been repeated on a different data set taken along the same orbit 2.5 seconds after the first survey. Since the satellite has moved only about 18Km during this time period, the parameter value should be very close to that estimated on the first data set. As a result we can expect to find the maximum of the Kurtosis in a correspondence of almost the same velocity v.

Figure 6 illustrates the plot of the Kurtosis for the second data set. A comparison of the two plots of Figure 5 and Figure 6 shows a difference of about 1.2m/sec. on the estimate of the "best" velocity v_o.

This difference could be partly or completely caused by a real parameter variation. Alternatively, it could be the precision limit of this method. The second hypothesis is much more probable. In fact, the only geometric change that can produce such a velocity variation in such a small time is the latitude change be-

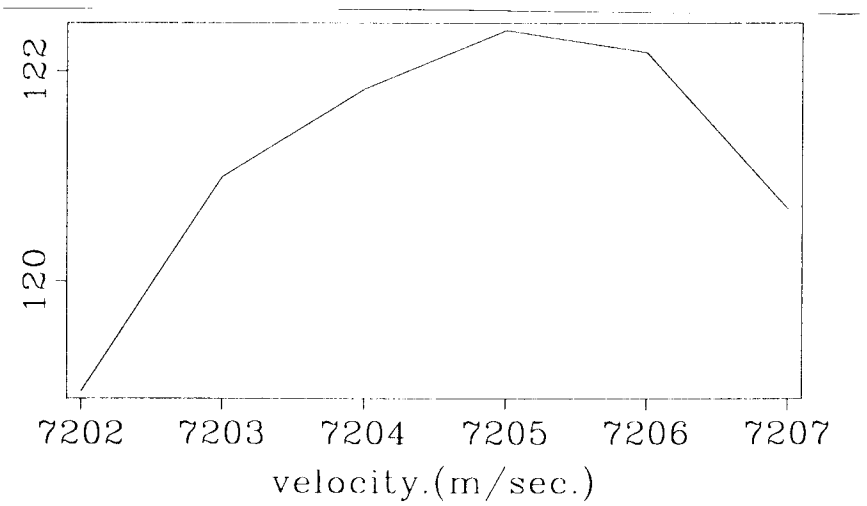

FIG. 6. Kurtosis vs. satellite velocity. Same measure as in Figure 5, but carried out on a data set taken 2.5 seconds after.

tween the two observed areas. Unfortunately, its effect would produce a velocity variation of opposite sign. (According to the satellites' effemerides, the latitude of the observed area passes from 43° to 43.16° and the earth's velocity component, in the along-track direction, from -87.48m/s to -86.62m/s).

In conclusion, we believe that this deconvolution technique may allow us to estimate the satellite velocity with a precision of about 4 parts over 10^4. This result is not completely satisfactory. Regardless, a different blind deconvolution technique proves to be much more precise than the one based on Kurtosis.

The residual focusing operator

The antenna aperture is very small if compared to seismic surveys (the survey angle of SEASAT SAR was about 1.3^0). Consequently, the residual operator, due to a small error in the focusing parameter, can be considered monodimensional. Taking advantage of this, let us analyze the image $d(x,z)$ that is obtained by applying equation (1) to the raw data with some incorrect velocity parameter v_m. (Here we recall that v_m is the satellite velocity and not the migration velocity whose value is half the velocity of light). The focused image $d(x,z)$ can be expressed as a monodimensional convolution between the sources $r(x,z)$ and the operator $O(x)$:

$$d(x,z) = r(x,z) * O(x) \tag{8}$$

An analytical representation of this operator can be carried out with some approximations by equation (1).

In fact, it can be shown (Rocca, 1987) that the focusing of SAR range compressed data can be carried out in two steps:

i) a wavenumber dependent time shift of the data

ii) a convolution in the x domain

Now, let us suppose to focus the SAR data using an incorrect velocity value $v_m = v_0 + v_e$.

Then, both the shift and the convolution operators will be incorrect. Nevertheless, if the velocity error v_e is much smaller than the correct velocity v_0, the defocusing effect due to the "convolution error" is much greater than the "shift error" (Rothman et al., 1985). The length of $g_e(x)$, the residual focusing operator, (Ottolini, 1988) can be found by exploiting the fact that the SAR signal is band limited in the wavenumber domain. In fact, the radar antenna beam has a small aperture θ in the azimuth direction and, apart from a constant value due to the earth rotation, the largest measured wavenumber is $k_{xo} = \omega_0 \sin\theta/c$. This allows us to use a finite value of the pulse repetition frequency (PRF) which is the sampling frequency in the x domain. If we assume that the measured signal had a maximum wavenumber equal to $PRF/2v_0$, then the focusing operator $G_0(k_x)$ and the residual one $G_e(k_x)$ must have the same maximum extension in the wavenumber domain. Consequently, assuming that the maximum wavenumber of the residual operator can be approximated with its maximum instantaneous frequency, the following relation holds:

$$x_M = \frac{\pi PRFcz_e}{v_0\omega_0}, \tag{9}$$

where x_M is the length of the residual operator. For example, in the case of SEASAT data the residual operator length which corresponds to a velocity error of one part over 1000 (v_e=7.5m/s) is about 47m, or 10 samples.

The cross-correlation method

A different technique can be now considered for blind deconvolution (Bellini and Rocca, 1988). The sampled residual operator can be written as: $O(i\Delta x)$ with $\Delta x = v_0/PRF$. The problem of finding the residual operator can be formalized as follows: the data r_k (the source field) that enter the filter with unknown pulse response are iid random variables with probability density $f_r(r)$. The output sequence y_k is obtained as follows:

$$y_k = r_k + \sum_i O(i\Delta x) r_{k-i}. \tag{10}$$

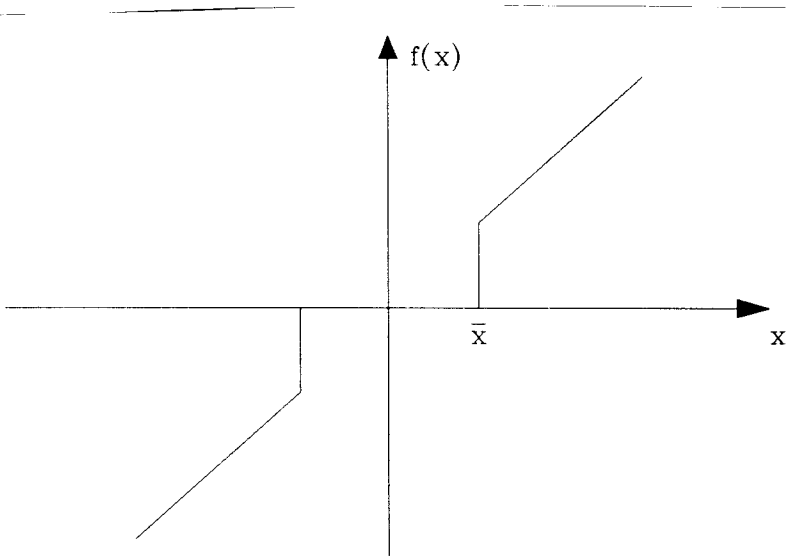

FIG. 7. Non-linear function used for the computation of γ_i.

Our goal is the retrieval of the coefficients $O(i\Delta x)$ using only the output sequence y_k, (the focused image), and the pdf of the input data. Bellini and Rocca have shown that the coefficients $O(i\Delta x)$ are proportional to the quantities

$$\gamma_i = \frac{1}{N}\sum_k \ell(y_k^*)y_{k-i}, \tag{11}$$

where $\ell(.)$ is a non-linear function that depends on the pdf of the input data as

$$\ell(y) = \frac{-f_r'(y)}{f_r(y)}. \tag{12}$$

This nonlinear function is optimal in the sense that it minimizes the variance of γ_i. Unfortunately, the SAR images do not have identical pdf; thus, a standard non-optimal $\ell(.)$ must be used. We have adopted a very simple function that is a good compromise between computational efficiency and performance quality. This function is plotted in Figure 7.

The computational efficiency of this nonlinearity is due to the fact that no multiplies are requested. In fact, depending on the absolute value of the datum, it can be set to zero or left unchanged. In our experiments, this non-linear function has been slightly modified to improve both the computational efficiency and performance quality. After the function of Figure 7 has been applied to the complex data, only the greatest sample among consecutive non-null samples has been taken. In

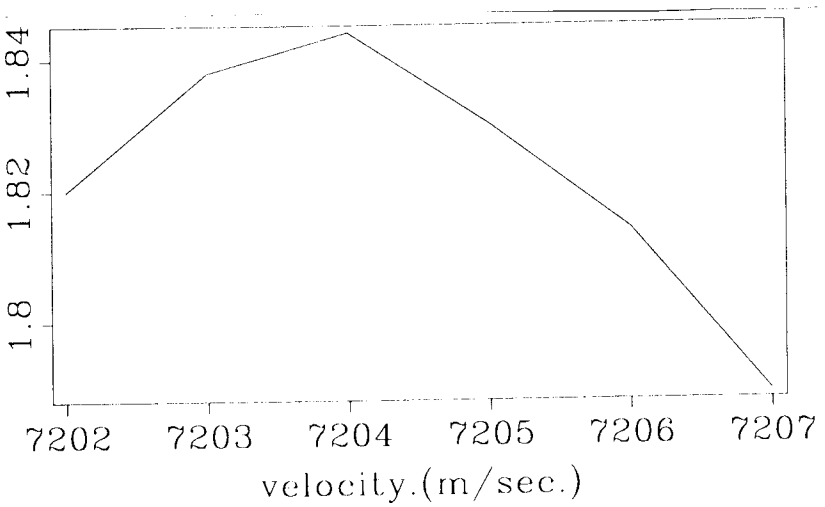

FIG. 8. $|\ \gamma_0\ |$ vs. the satellite velocity. The measure has been carried out on a SEASAT image (4096x256).

this way, the number of multiplies requested by equation (11) is strongly reduced, and a smaller weight is given to smaller data.

From equation (11) the three values γ_{-1}, γ_0 and γ_1 have been computed on SEASAT SAR images focused with different satellite velocities. This is similar to the Kurtosis computation.

Amplitude of the central value

Let us first analyze the behavior of $|\ \gamma_0\ |$. It is easy to see that the absolute value of γ_0 computed with the chosen non-linear function is proportional to the average image energy at the estimated source position. Consequently, the absolute value of γ_0 will be greater for smaller velocity errors. This simple analysis has been confirmed by the experimental results shown in Figures (8) and (9).

Note that in this case the results obtained on the two SEASAT SAR data sets are more consistent than those of the Kurtosis computation. The velocity value that corresponds to the maximum of $|\ \gamma_0\ |$ is very close to that computed in the previous section, but the velocity difference between the two data sets is now consistent with the latitude displacement between the two observed areas. In this case, the satellite velocity can be estimated with a precision better than 1 part over 10,000.

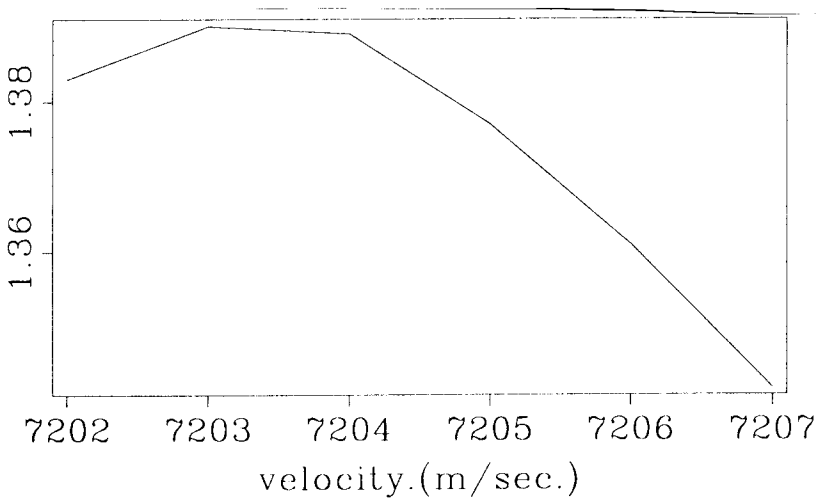

FIG. 9. $|\gamma_0|$ vs. the satellite velocity. Same measure as in Figure 8, but carried out on a data set taken 2.5 seconds after.

The sign of the error

Exploiting the phase of γ_{-1} and γ_1, it is now possible to find the sign of the velocity error. In fact, if we approximate the operator $O(i\Delta x)$ with the error operator $g_e(i\Delta x)$, the phases of γ_{-1} and γ_1 will be proportional to the quadratic phase of the theoretical error operator apart from some linear phase component due to the earths' rotation and/or the antenna squint angle. Figure (10) plots the theoretical behavior of $\angle\gamma_{-1} + \angle\gamma_1$ vs. the velocity error v_e.

It is obvious that in this case, the velocity error (both sign and amplitude, could be directly derived by the measured quantity. Nonetheless, because of the low-pass effect on $g_e(i\Delta x)$, the theoretical behavior of $\angle\gamma_{-1} + \angle\gamma_1$ differs from that shown in Figure (10) especially around the smallest velocity errors as shown in Figure (11).

From this figure, it is clear that the correct satellite velocity corresponds to the zero of the plotted curve. Unfortunately, the same value of $\angle\gamma_{-1} + \angle\gamma_1$, apart from zero can be associated to two different values of the velocity error v_e. Its sign is always consistent with that of the velocity error however. Consequently, it is possible to modify the focusing parameter repeatedly, thus making it closer to correct value.

To confirm this analysis, the measure of $\angle\gamma_{-1} + \angle\gamma_1$ has been carried out on real SEASAT SAR images for different parameter values. The resulting plot is shown

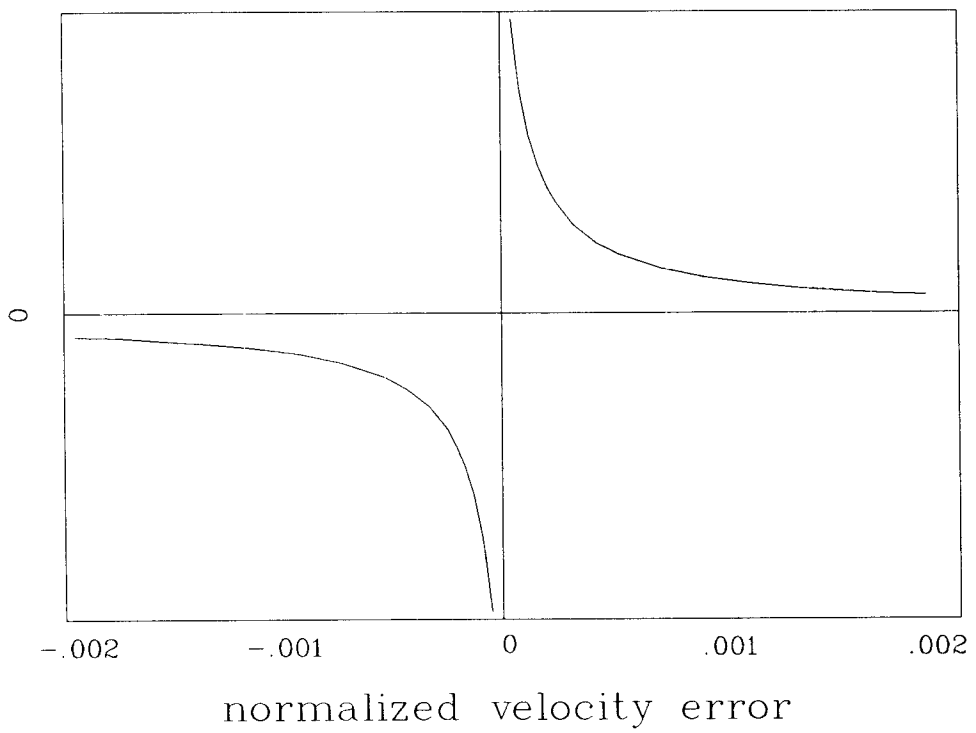

FIG. 10. Theoretical behavior of residual operator phase vs. velocity error v_e.

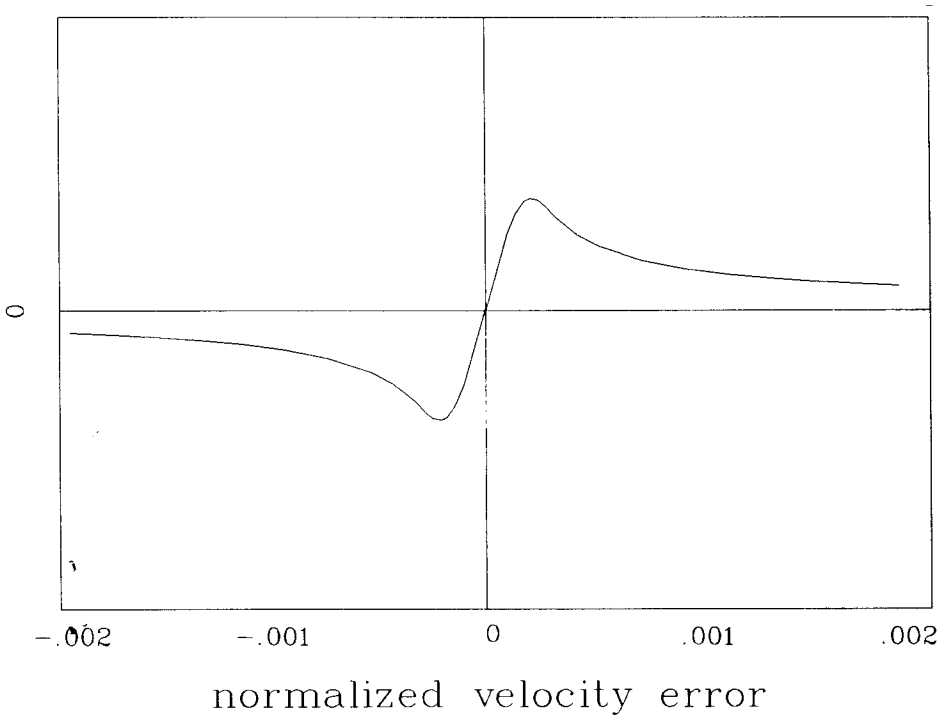

FIG. 11. Low-passed residual operator phase vs. the velocity error v_e.

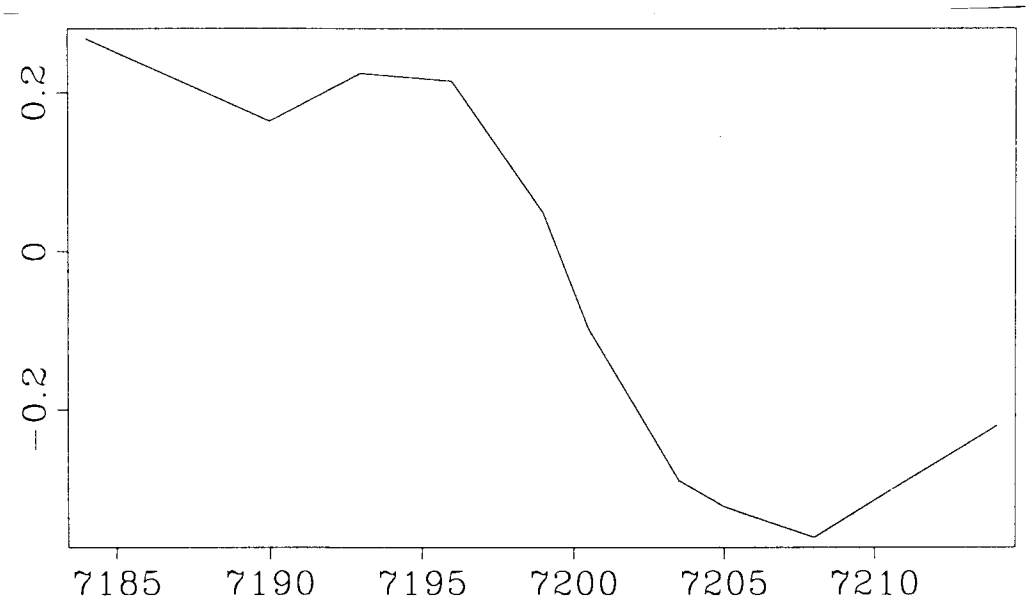

FIG. 12. Experimental measure of residual operator phase vs. satellite velocity.

in Figure 12. This curve has the predicted shape; its zero value is reached in a correspondence of the velocity which produces the greatest value of γ_0.

CONCLUSIONS

An autofocusing technique for SAR images has been presented. It has been shown that the measurement of the two parameters involved in the focusing process can be carried out by measuring only one parameter on two data subsets centered at different ranges. The blind deconvolution technique described by Bellini (1988) has been applied to SAR images focused with incorrect parameter values. The parameter error sign can be immediately measured, whereas the information about its absolute value is ambiguous. Nonetheless, if the same measure is repeated on the same data set focused with a different parameter value, this ambiguity can be removed. Precision better than one part over 10,000 of the focusing parameter value has been obtained with this autofocusing technique.

REFERENCES

Bellini, S. and Rocca, F., 1988, Near optimal blind deconvolution: ICASSP-88.

Fitch, J. P., 1988, Synthetic Aperture Radar: Springer Verlag, New York, 1988.

Ottolini, R., 1988, Interactive residual synthetic aperture radar imaging: SEP–**57**.

Rocca, F., 1987, Synthetic Aperture Radar: a new application for wave equation techniques: SEP–**56**, 167–189.

Rothman, D., Levin, S., and Rocca, F., 1985, Residual migration: applications and limitations: Geophysics, **50**, 110 - 126.

Wiggins, R.A., 1977, Minimum Entropy Deconvolution: Geoexploration, **16**, 21-35.